

Optical probing of mechanical loss of a Si_3N_4 membrane below 100 mK

R. Fischer,^{1,*} N. S. Kampel,¹ G. G. T. Assumpção,¹ P.-L. Yu,^{1,†}
K. Cicak,² R. W. Peterson,¹ R. W. Simmonds,² and C. A. Regal^{1,‡}

¹*JILA, National Institute of Standards and Technology and University of Colorado, and Department of Physics, University of Colorado, Boulder, Colorado 80309, USA*

²*National Institute of Standards and Technology, 325 Broadway, Boulder, Colorado 80305, USA*
(Dated: April 30, 2019)

We report on low mechanical loss in a high-stress silicon nitride (Si_3N_4) membrane at temperatures below 100 mK. We isolate a membrane via a phononic shield formed within a supporting silicon frame, and measure the mechanical quality factor of a number of high-tension membrane modes as we vary our dilution refrigerator base temperature between 35 mK and 5 K. At the lowest temperatures, we obtain a maximum quality factor (Q) of 2.3×10^8 , corresponding to a Q -frequency product (QFP) of 3.7×10^{14} Hz. These measurements complement the recent observation of improved quality factors of Si_3N_4 at ultralow temperatures via electrical detection. We also observe a dependence of the quality factor on optical heating of the device. By combining exceptional material properties, high tension, advanced isolation and clamping techniques, high-stress mechanical objects are poised to explore a new regime of exceptional quality factors. Such quality factors combined with an optical probe at cryogenic temperatures will have a direct impact on resonators as quantum objects, as well as force sensors at mK temperatures.

Stoichiometric silicon nitride (Si_3N_4) films are a unique material in the field of nanomechanics due to their high internal stress that enables high mechanical quality factors along with high resonance frequencies. Thus far, silicon-nitride based resonators have been found to be favorable devices for studying quantum optomechanical phenomena [1], precision force sensing applications [2, 3], and bidirectional microwave-optical transducers [4–6]. These applications harness extremely high quality factors that are required for observing quantum coherent effects and for precision sensing. The key to the unique nature of membrane mechanics is that stress provides relatively high resonance frequencies, while maintaining low dissipation rate [7].

Although numerous studies have focused on both internal and external loss mechanisms governing the quality factors of Si_3N_4 -based resonators, the ultimate limit to the QFP has not been identified, especially at cryogenic temperatures [7–13]. Specifically, a stringent upper bound for Q , set by thermoelastic damping of Si_3N_4 , is particularly high, reaching 3×10^{11} at room-temperature [8, 14]. Recently, a square SiN membrane device operated at 20 mK with an electrical readout demonstrated Q 's above 10^8 for a mode frequency of about 250 kHz [15]. Their observed increase in Q with decreasing temperature (below 1 K) was consistent with previous observations of decreased internal mechanical loss in amorphous solids with temperature [16]. Recently, it was also shown that by decreasing the external radiation losses as well as the edge clamping losses, room temperature Si_3N_4 can approach and surpass quality factors of 10^8 for trampoline and phononic crystal shield designs [13, 17, 18]. By combining the suppression of internal losses through cryogenic temperatures with advanced designs for isolating the resonator to reduce external losses,

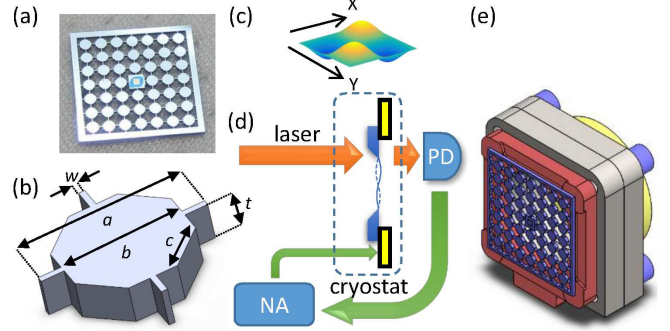


FIG. 1. (color online) (a) A illustration of the fabricated sample composed of phononic crystal silicon chip with the Si_3N_4 membrane resonator at the center. The periodic structure is comprised of large area pads connected by thin bridges. The membrane is separated from the PnC by a membrane frame support, while the entire chip is surrounded by a chip frame. (b) Schematic of a PnC unit cell and definitions of the geometry parameters. See Table I for the values of these parameters. (c) Illustration of the (2,2) membrane mode. (d) Schematic sketch of the apparatus to measure mechanical decay time via a ringdown technique. A laser beam is transmitted through the membrane (blue), which is mounted inside the dilution refrigerator (dashed blue). The transmitted beam is detected by an amplified photodiode (PD). The membrane modes are excited by a piezo ring (yellow) epoxied onto the sample. The excitation and narrowband filtering of the optical detection is done by a network analyzer (NA). (e) Sample assembly. The sample (blue) is mounted on a silicon holder (red), which is mounted on two invar steel adapters (gray). These adapters are epoxied to the piezo actuator (yellow). The thermal link of the assembly to the base-plate is completed with a copper foil (not-shown) pressed between the invar adapters.

further improvements to Q seem possible.

Here we study the mechanical loss of a MHz frequency

Si_3N_4 membrane at temperatures down to 35 mK using piezoelectric excitation and optical detection. We show that the mechanical loss decreases significantly below 5 K, reaching a maximal measured Q of 2.3×10^8 for a mode frequency of 1.6 MHz, corresponding to a QFP of 3.7×10^{14} Hz. Additionally, the observed quality factors were sensitive to optical probing power, further emphasizing the role of the thermal environment in the mechanical dissipation.

The sample we utilize is a high stress (0.8 GPa) square membrane resonator surrounded by a phononic crystal (PnC) shield. The sample is depicted in Fig. 1(a, b), with the parameter values listed in Table I. The devices are created starting with a high stress Si_3N_4 film 100 nm thick grown by low pressure chemical vapor deposition (LPCVD) on a 300 μm silicon wafer. The final sample chip is a 10 mm x 10 mm square, with the released Si_3N_4 membrane in the center. The main aspects of the fabrication process are reported in [19]. In brief, the membrane is created through a combination of deep reactive ion etching (DRIE), and a final KOH etch to release the membrane. The PnC structure is created by etching all the way through the silicon with DRIE; during the PnC creation the membrane is protected by process adhesive that, for the devices reported here, filled the entire back trench of the released membrane, improving yield. Further, membrane cleanliness was improved by removing the Si_3N_4 film on the membrane side of the device (outside of the suspended membrane region) prior to creating the PnC. While the device fabrication is similar to previous work [19], there are several important design changes to the PnC which should improve the robustness and reproducibility of the band-gap, see Fig. 1(b). These improvements include narrowing the width of the bridges (47 μm compared to 97 μm in the previous design) to increase the phononic isolation and designing chamfered corners to better reproduce simulated structures in the fabrication. The design band-gap of the PnC with the dimensions listed in Table I spans between 1.1-2.1 MHz, and between 3.1-3.3 MHz. The band-gaps were calculated using Comsol, as described in detail in [19].

The experimental setup to measure the mechanical quality factor is depicted in Fig. 1(d, e). The sample is anchored to the base of a dilution refrigerator, and light is directed to the membrane through a narrow cryogenic beam path designed to filter 300 K blackbody radiation [20]. The laser beam was generated by a diode with a 900 nm wavelength, and detected by either a Si avalanche or an InGaAs amplified photodiode. An interferometric signal which monitors the position of the membrane is created due to a low finesse cavity between the membrane and a low reflectivity mirror inside the cryostat [8, 21]. Mechanical driving was applied by a piezoelectric ring (Noliac NAC2124). The mechanical ringdown measurements were performed with a network analyzer (HP 4395A), where a continuous wave excitation of the

TABLE I. Measured geometry parameters of the devices

Definition	symbol	Device
chip size		10 mm
number of unit cells		4
unit cell size	a	1275 μm
block length	b	925 μm
bridge width	w	47 μm
wafer thickness	t	300 μm
membrane length		516 μm
chamfer size	c	$\sqrt{2} \times 275 \mu\text{m}$
membrane frame size		1125 μm
chip frame size		500 μm
membrane thickness		0.1 μm

piezoelectric ring at a specific membrane mode frequency was stopped abruptly and the decay of the mechanical oscillation was optically monitored via the interferometric signal. We measure the mechanical decay time constant from the ringdown data τ_m , and extract the mechanical loss rate $\Gamma_m = (2\pi\tau_m)^{-1}$. The quality factor of mode m , Q_m is the ratio of the mechanical angular frequency Ω_m , and the loss rate Γ_m , $Q_m = \Omega_m/\Gamma_m$.

To study the temperature dependence of Q , we varied the base-plate temperature of the refrigerator from 35 mK to 5 K. The base-plate temperature was measured with a calibrated RuO_2 resistive thermometer. The thermal link of the membrane to the base-plate is achieved with a copper foil pressed between the invar adapters, shown in Fig. 1(e). The thermalization efficiency down to 120 mK was confirmed by an independent measurement performed on the same setup and sample, utilizing a 1064 nm resonant high finesse cavity to probe the thermally-induced brownian motion of a membrane. There we obtained the thermal phonon occupancy via optomechanical relations [22] and found good agreement with the base-plate temperature down to 120 mK [23].

At each temperature, we measured the mechanical Q of a few membrane modes that displayed values higher than 10^6 . These mode frequencies were inside the design band-gap of the PnC. Other modes that were outside of the band-gap of the PnC displayed values lower than 10^5 . As expected, the decrease in the base-plate temperature resulted in an increase in the value of Q (Fig. 2(a)), and correspondingly a decrease in the loss rate Γ_m (Fig. 2(b)). In these data, we witness a leveling-off of the Q -values at the low end of the temperature range. The leveling-off of the Q between 200 mK to 1 K, does not occur here, in contrast to the results in [15], and continues to drop above 1 K, similar to the results of [8]. To make this feature of the data more apparent, we plot the difference in the loss rate Γ_m from that at 35 mK in Fig. 2(b). Notice that this quantity increases monotonically above 100 mK

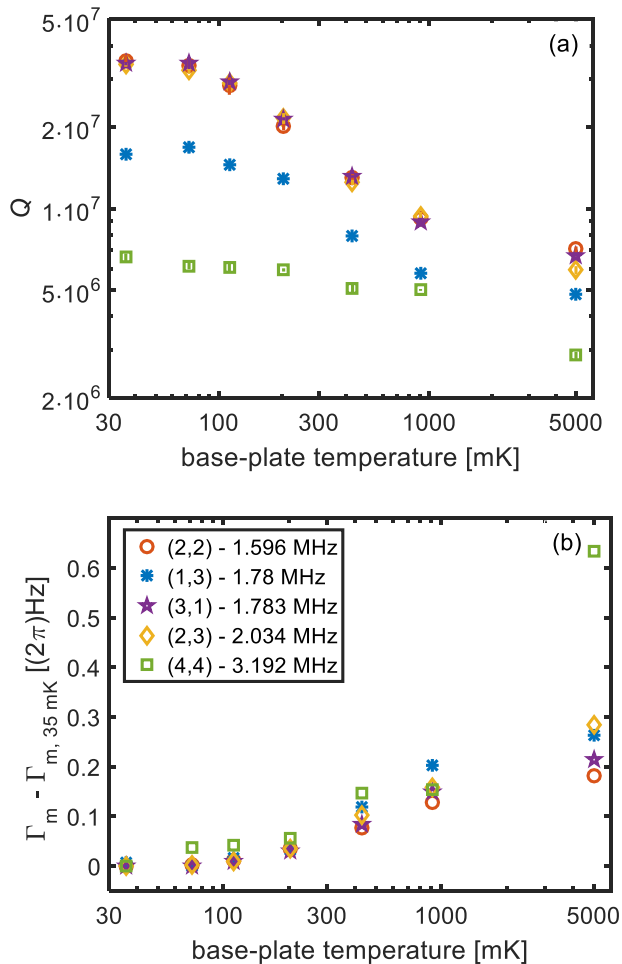


FIG. 2. Measurements of Q -factor (a) and difference in loss rate from minimal loss at 35 mK (b) of multiple membrane modes versus base-plate temperature and at an optical power 1 nW. Errorbars are standard deviation of repeated measurements.

For the above measurements, we used a free space optical probe near 900 nm, operated continuously. By varying the probe's optical power we examined its effect on the resonator's dissipation. As we increase the probe's optical power, we find that the mechanical quality factor decreases significantly (Fig. 3), presumably due to heating resulting from optical absorption. While we do expect that heating effects become more important with the decrease of thermal conductivity of amorphous solids below 1 K [16, 24, 25], we stress that the measurements here do not represent a quantitative study of the optical properties of Si_3N_4 itself at cryogenic temperatures; for example, we have not characterized the spatial mode of the optical spot on the membrane. We note the effective power of a 1064 nm beam, probing an optical cavity displaying heating effects, was measured to be considerably higher than for the 900 nm optical probe power for which we see an effect here. Specifically, previous work shows

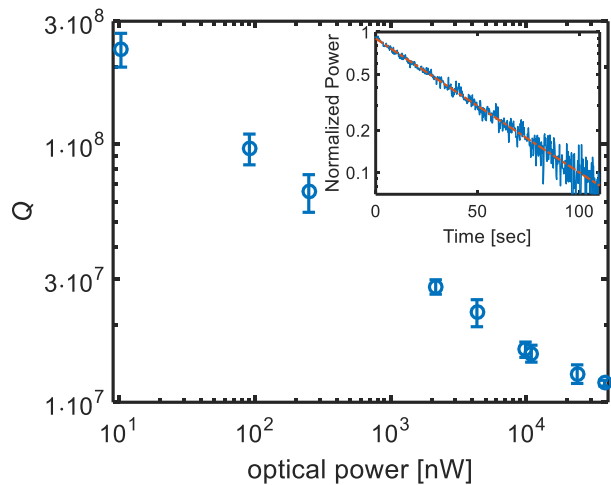


FIG. 3. Mechanical ringdown results at a base-plate temperature of 35 mK versus input laser power measured via free-space optical probe at 900 nm. The errorbars are calculated from repeated measurements at the same laser power. Inset: Mechanical ringdown of mode (2,2) at a laser power of 10 nW (blue), and an exponential fit with a decay rate of $\Gamma_m = (2\pi) 7.05 \pm 0.005$ mHz. Errorbars are standard deviation of repeated measurements.

no heating effects at 120 mK [23], and a heat transfer analysis at 35 mK indicates much smaller optical effects than those shown in Fig. 3 would cause significant effects to the Si_3N_4 alone. Further, we note that optical excitation effect on mechanical quality factor is a complex subject, which cannot be simply described by a heating of a thermal bath [26]. With the data at hand, a complete picture cannot be discerned. The study of optical properties of Si_3N_4 membranes will be the subject of a future study.

Nonetheless, the Q dependence on optical absorption is indicative of variation of an internal dissipation as a function of temperature. Salient features we observe are that at a minimal probe power of 10 nW, and temperature of 35 mK, we find a maximal measured Q of $2.3 \pm 0.3 \times 10^8$ for the (2,2) mode, corresponding to a QFP of 3.7×10^{14} Hz as seen in Fig. 3. The error bar shown is dominated by the low signal to noise level at the light level of the probe. We note the Q values of Fig. 3 are higher than the values depicted in Fig. 2 and were obtained prior to thermal cycling of the refrigerator. We suspect that the thermal cycling resulted in an added loss that obscured the reduction in dissipation below 100 mK in the data of Fig. 2.

In conclusion, we optically probed the mechanical loss of MHz frequency Si_3N_4 membranes down to mK temperatures. The highest Q we measured was 2.3×10^8 at 35 mK, corresponding to a QFP of 3.7×10^{14} Hz, the highest value achieved for Si_3N_4 resonators so far. These results push further the performance of these resonators

at cryogenic temperatures, both for quantum studies, as well as for precision measurements. A next step would be to combine cryogenic low-loss membrane resonator with additional geometric design features aiming to further reduce internal and external loss channels to reach even higher levels of isolation. Finally, the low thermal conductivity and the high- Q of Si_3N_4 membranes at mK temperatures allows optical heating effects to be measured. This enables a quantitative study of optical properties of Si_3N_4 membranes.

We thank A. Higginbotham for technical assistance. This work was supported by AFOSR PECASE, ONR DURIP, AFOSR-MURI, Rafael Ltd., the Cottrell Scholar's program, and the National Science Foundation under grant number 1125844.

Contributions from NIST are not subject to U.S. copyright. Reference to specific products and services does not constitute endorsement by NIST. Other vendors may provide equivalent or better products.

* ran.fischer@jila.colorado.edu

† Current address: School of Electrical and Computer Engineering, Birck Nanotechnology Center, Purdue University, West Lafayette, IN 47907 USA

‡ regal@colorado.edu

- [1] J. Thompson, B. Zwickl, A. Jayich, F. Marquardt, S. Girvin, and J. Harris, *Nature* **452**, 72 (2008).
- [2] E. Gavartin, P. Verlot, and T. J. Kippenberg, *Nature nanotechnology* **7**, 509 (2012).
- [3] N. Scozzaro, W. Ruchotzke, A. Belding, J. Cardellino, E. Blomberg, B. McCullian, V. Bhallamudi, D. Pelekhov, and P. Hammel, *Journal of Magnetic Resonance* **271**, 15 (2016).
- [4] J. Bochmann, A. Vainsencher, D. D. Awschalom, and A. N. Cleland, *Nature Physics* **9**, 712 (2013).
- [5] R. W. Andrews, R. W. Peterson, T. P. Purdy, K. Cicak, R. W. Simmonds, C. A. Regal, and K. W. Lehnert, *Nature Physics* **10**, 321 (2014).
- [6] T. Bagci, A. Simonsen, S. Schmid, L. G. Villanueva, E. Zeuthen, J. Appel, J. M. Taylor, A. Sorensen, K. Usami, A. Schliesser, and E. S. Polzik, *Nature* **507**, 81 (2014).
- [7] Q. P. Unterreithmeier, T. Faust, and J. P. Kotthaus, *Phys. Rev. Lett.* **105**, 027205 (2010).
- [8] B. M. Zwickl, W. E. Shanks, A. M. Jayich, C. Yang, A. C. B. Jayich, J. D. Thompson, and J. G. E. Harris, *Applied Physics Letters* **92**, 103125 (2008).
- [9] I. Wilson-Rae, R. Barton, S. Verbridge, D. Southworth, B. Ilic, H. Craighead, and J. Parpia, *Phys. Rev. Lett.* **106**, 047205 (2011).
- [10] P.-L. Yu, T. P. Purdy, and C. A. Regal, *Phys. Rev. Lett.* **108**, 083603 (2012).
- [11] S. Chakram, Y. S. Patil, L. Chang, and M. Vengalattore, *Phys. Rev. Lett.* **112**, 127201 (2014).
- [12] A. H. Ghadimi, D. J. Wilson, and T. J. Kippenberg, arxiv:1603.01605v1.
- [13] Y. Tsaturyan, A. Barg, E. S. Polzik, and A. Schliesser, arXiv:1608.00937 (2016).
- [14] A. N. Norris and D. M. Photiadis, *The Quarterly Journal of Mechanics and Applied Mathematics* **58**, 1 (2006).
- [15] M. Yuan, N. A. Cohen, and G. A. Steele, *Appl. Phys. Lett.* **107** (2015).
- [16] R. O. Pohl, X. Liu, and E. Thompson, *Rev. Mod. Phys.* **74**, 991 (2002).
- [17] R. A. Norte, J. P. Moura, and S. Groblacher, *Phys. Rev. Lett.* **116** (2016).
- [18] C. Reinhardt, T. Muller, A. Bourassa, and J. Sankey, *Phys. Rev. X* **6** (2016).
- [19] P.-L. Yu, K. Cicak, N. S. Kampel, Y. Tsaturyan, T. P. Purdy, R. W. Simmonds, and C. A. Regal, *Appl. Phys. Lett.* **104**, 023510 (2014).
- [20] A. G. Kuhn, J. Teissier, L. Neuhaus, S. Zerkani, E. van Brackel, S. Deléglise, T. Briant, P.-F. Cohadon, A. Heidmann, C. Michel, L. Pinard, V. Dolique, R. Flaminio, R. Taïbi, C. Chartier, and O. L. Traon, *Appl. Phys. Lett.* **104**, 044102 (2014).
- [21] D. J. Wilson, *Cavity Optomechanics with High-Stress Silicon Nitride Films*, Ph.D. thesis, California Institute of Technology (2012).
- [22] R. W. Peterson, T. P. Purdy, N. S. Kampel, R. W. Andrews, P.-L. Yu, K. W. Lehnert, and C. A. Regal, *Phys. Rev. Lett.* **116**, 063601 (2016).
- [23] N. S. Kampel, R. W. Peterson, R. Fischer, P.-L. Yu, K. Cicak, R. W. Simmonds, K. W. Lehnert, and C. A. Regal, arXiv:1607.06831 (2016).
- [24] M. M. Leivo and J. P. Pekola, *Appl. Phys. Lett.* **72**, 1305 (1998).
- [25] D. J. Wilson, V. Sudhir, N. Piro, R. Schilling, A. Ghadimi, and T. J. Kippenberg, *Nature* **524**, 325 (2015).
- [26] A. G. Krause, J. T. Hill, M. Ludwig, A. H. Safavi-Naeini, J. Chan, F. Marquardt, and O. Painter, *Phys. Rev. Lett.* **115**, 233601 (2015).